Geodesic Motion in Trivializable Gauge Fields

T. Heck and M. Sorg

Institut für Theoretische Physik, Universität Stuttgart

Z. Naturforsch. **46a**, 655–668 (1991); received October 5, 1989

The geodesic problem is studied for a Riemannian structure, which is generated by an SO(4) trivializable gauge field. The topological and elliptic geometric defects of such a structure act as attractors for the geodesic curves.

Key words: Field theory, Riemannian geometry, Geodesics, Trivializable gauge fields, Merons.

I. Introduction

It has been demonstrated in some recent papers [1–3] that SO(4) trivializable gauge fields are able to induce a Riemann-Cartan structure over the Euclidean base space E_4. The fundamental object of such a specific geometric structure is the characteristic distribution $\widehat{\Delta}$ which yields a unique $(1+3)$-splitting of the base space. In contrast to this, such a splitting is of some arbitrariness when one considers a general Riemann-Cartan structure [4]. On the other hand, one can also construct directly a Riemannian space by considering the distribution $\widehat{\Delta}$ as a dynamical object obeying a certain set of first order field equations [5].

In any case, the characteristic distribution essentially determines the Riemann-Cartan structure of trivializable gauge fields and therefore suggests itself for a more detailed investigation of its interrelationship with such a geometric structure. The present paper deals with the geodesic aspect of that relationship. We restrict ourselves to the case where $\widehat{\Delta}$ is integrable, which admits the introduction of a strictly Riemannian structure. The latter one may be conveniently visualized by its characteristic network consisting of the integral surfaces of $\widehat{\Delta}$ (*characteristic surfaces*) and its orthogonal lines (*characteristic lines*) which simultaneously are geodesics of the Riemannian metric **G** [6]. By this fact, one may suppose that there is a close relationship between the defect of the characteristic network and the geodesics.

Indeed, the nature of such a relationship is readily recognized by considering a simple example: the application of the present geometric theory to the well-known dimeron configuration [7, 8] demonstrates that the topological charges are attractors of the geodesics, i.e. any geodesic terminates at one of the two defect locations, where the topological charge is concentrated [3]. Clearly, we take this result as a sufficient motivation for a closer inspection of this effect. Our procedure is the following:

First we give a short survey over the Riemannian structure, induced by trivializable gauge fields, with emphasis upon the ocurrence of defects and their meaning for the geodesic curves (Section II). Next, we specify the general geometric structure to the SO(3) symmetric case because for this symmetry one can find exact solutions of the geodesic problem (Section III). Then we further specify the general SO(3) symmetric configurations to a special subcase which, on the one hand, is simple enough to be treated exactly and, on the other hand, is able to comprehend various types of defects; this is the generalized dimeron configuration (Section IV). Finally, we exactly solve the geodesic problem for the generalized dimeron configuration, thus establishing the expected result which says that topological and elliptic geometric defects are attractors for the geodesic lines.

The present work may be understood as a further demonstration of the intimate relationship between the traditional Riemannian geometry and modern gauge theories; for a historic synopsis of both lines of thinking the reader is referred to [13].

II. The Geodesic Problem

There are various pecularities inherent in the Riemannian structure which is generated by a trivial-

Reprint requests to Dr. M. Sorg, II. Institut für Theoretische Physik der Universität Stuttgart, Pfaffenwaldring 57, D-7000 Stuttgart 80.

0932-0784 / 91 / 0800-0655 $ 01.30/0. – Please order a reprint rather than making your own copy.

izable gauge field. In the following we exclusively deal with the *geodesic aspect*. Especially, we shall concentrate ourselves upon the defects of the Riemannian structure and their influence upon the geodesic curves.

II.1. Riemannian Structure

One of the most striking features is the natural $(3+1)$-decomposition of the Riemannian structure [3], which in the present case is automatically produced by the very generation mechanism. According to this mechanism, the Riemannian metric **G** is split naturally into a "space part" $\mathscr{B}$ and its "time-like" complement [9]:

$$G_{\mu\nu} = \mathscr{B}_{\mu\nu} - p_\mu p_\nu \,. \tag{II.1}$$

Here, the first term ($\mathscr{B}$) is the covariant projector onto the characteristic surfaces

$$\begin{aligned} (G^{-1})^{\nu\sigma}\, \mathscr{B}_{\mu\nu}\, \mathscr{B}_{\sigma\lambda} &= \mathscr{B}_{\mu\lambda}\,, \quad \text{(a)} \\ \mathscr{B}_{\mu\nu}\, p^\nu &= 0\,. \qquad \text{(b)} \end{aligned} \tag{II.2}$$

It is composed of the extrinsic curvature **B** of the characteristic surfaces

$$\mathscr{B}_{\mu\nu} = c^2\, B_{i\mu} B^i{}_\nu \,, \tag{II.3}$$

where we have introduced for convenience a constant length parameter c. **B** itself is covariantly constant

$$\mathscr{D}_\lambda B_{i\mu} = 0\,. \tag{II.4}$$

This, together with the constancy of the characteristic vector $\boldsymbol{p}$

$$\nabla_\lambda p_\mu = 0\,, \tag{II.5}$$

implies the usual constraint upon the Riemannian metric **G** (II.1)

$$\nabla_\lambda G_{\mu\nu} = 0\,. \tag{II.6}$$

The Riemannian **R** itself acquires the very simple shape

$$R_{\mu\nu\sigma\lambda} = -\frac{1}{c^2}\left[\mathscr{B}_{\mu\sigma}\, \mathscr{B}_{\nu\lambda} - \mathscr{B}_{\mu\lambda}\, \mathscr{B}_{\nu\sigma}\right] \tag{II.7}$$

and thus must be constant on account of (II.4),

$$\nabla_\varrho R_{\mu\nu\sigma\lambda} = 0\,. \tag{II.8}$$

In this way, the characteristic surfaces are equipped with a homogeneous and isotropic 3-geometry, which translates to a Riemannian 4-geometry of constant curvature.

II.2. Two Types of Defects

A futher peculiarity of the geometric structure described above is the fact that it always must contain some defect. Since these defects play an important part for the geodesic problem, we are going into some detail for their definition.

First, we have to discern between two types of defects: the *topological* and the *geometric* defects. Both defects refer, respectively, to a certain type of degeneration of the characteristic network. The topological type is associated to a source-like singularity of the characteristic lines and therefore is accompanied by a non-vanishing defect charge Q. On the other hand, the geometric defect type is associated to a vortex-like singularity and therefore has vanishing defect charge ($Q=0$).

Here, the computation of the defect charge Q is based upon the Gauß current **j** which is defined via its Poincaré dual $*j$ as

$$*j_{\mu\nu\lambda} = \frac{1}{2\pi^2}\, \varepsilon^{ijk} B_{i\mu}\, B_{j\nu}\, B_{k\lambda}\,. \tag{II.9}$$

From this 3-form one obtains the corresponding current vector j^σ as

$$\begin{aligned} j^\sigma &= \frac{1}{3!}\, \varepsilon^{\mu\nu\lambda\sigma}\, *j_{\mu\nu\lambda}\,, \\ \left(\varepsilon^{\mu\nu\lambda\sigma} &= \frac{1}{\sqrt{G}}\,[\mu, \nu, \lambda, \sigma]\right), \end{aligned} \tag{II.10}$$

where the brackets [...] denote the ordinary permutation symbol. Because of the covariant constancy of the extrinsic curvature (II.4), the Gauß current **j** is also constant,

$$\nabla_\varrho j^\sigma = 0\,. \tag{II.11}$$

Therefore it is expected to be proportional to the characteristic vector $\boldsymbol{p}$ (cf. (II.5)). Indeed, a simple calculation yields

$$j^\sigma = -\frac{1}{2\pi^2 c^3}\, p^\sigma \,, \tag{II.12}$$

which reveals the characteristic lines as the flux lines of the Gauß current **j**. For this reason, a defect charge Q may be associated to any defect structure of the characteristic lines by the following integral over some 3-cycle C^3 enclosing the defect set:

$$Q = \oint_{C^3} *j\,. \tag{II.13}$$

A simple example for such a topological defect is given by the well-known dimeron configuration, which exhibits two point charges of opposite sign ($Q = \pm \frac{1}{2}$).

In contrast to this, the *geometric* defect has $Q = 0$ and rather refers to the degeneration of the surface metric $\mathscr{B}$ (II.3). Its precise definition is based upon the existence of a tangent vector $\boldsymbol{b}$ of the characteristic surfaces ($p^\mu b_\mu = 0$), which annihilates the extrinsic curvature at the defect points

$$B_{i\mu} b^\mu = 0 . \tag{II.14}$$

Since the **B** field may be expressed by the representative tetrad $\{\hat{\boldsymbol{n}}, \boldsymbol{e}_i\}$ as

$$B_{i\mu} = -(\boldsymbol{e}_i \cdot \partial_\mu \hat{\boldsymbol{n}}) , \tag{II.15}$$

a geometric defect will occur whenever the unit vector $\hat{\boldsymbol{n}}$ becomes stationary along the tangent vector $\boldsymbol{b}$. If one regards the topological charge Q (II.13) as the winding number of the map $[\hat{n}]: C^3 \to S^3$, which takes the 3-cycle C^3 into the 3-sphere S^3 and is mediated by the unit vector $\hat{\boldsymbol{n}}$, then it becomes evident that a topological defect must necessarily occur whenever a geometric defect does not exist! Thus, any trivializable field configuration will exhibit at least one of the two types of defects.

II.3. Geodesics

According to the very simple geometric structure of the Riemannian space, described above, the corresponding geodesic equation

$$\frac{\mathrm{d}^2 x^\lambda}{\mathrm{d}s^2} + \Gamma^\lambda{}_{\mu\nu} \frac{\mathrm{d}x^\mu}{\mathrm{d}s} \frac{\mathrm{d}x^\nu}{\mathrm{d}s} = 0 \tag{II.16}$$

also admits some simple solutions. First observe that the characteristic lines themselves are geodesics on account of (II.5). Next verify also by means of that equation that a geodesic starting tangent to a characteristic surface is contained totally in this surface.

However, in the more general case of an arbitrary geodesic there arise some interesting questions: the geodesic motion in the dimeron field [3] has shown that the topological point defects act as attractors for the geodesic curves. Therefore one wants to know whether this attractive property of the topological defects is a special feature of the dimeron configuration or whether it is encountered for a quite general field configuration? The next question would refer to the geometric defects; are they also attractors? If yes, is there some difference with respect to the topological attractors? How does a geodesic run through a field containing both types of defects?

It seems hard to settle these questions in the quite general case, but we are able to manage some simplified situation which gives some hint how the general answer could look like. Our simplified procedure exploits the fact that the restriction of the curvature 2-form **R** (II.7) onto a 2-dimensional submanifold, generated by the characteristic vector $\boldsymbol{p}$ and some tangent **b** to the characteristic surfaces, vanishes,

$$R_{\mu\nu\sigma\lambda} p^\sigma b^\lambda = 0 . \tag{II.7}$$

If we therefore restrict the geodesic problem to this submanifold, we can parametrize it by "Cartesian coordinates" $\{\xi, \varkappa\}$ such that [10]

$$\begin{aligned} p_\mu &= c\, \partial_\mu \xi = \psi \hat{p}_\mu , \quad \text{(a)} \\ b_\mu &= \partial_\mu \varkappa , \quad \text{(b)} \end{aligned} \tag{II.18}$$

and then the geodesic problem reduces to its Euclidean analogue, which is solvable trivially in Cartesian coordinates. In this way, we can renounce a direct integration of the geodesic equation (II.16) and are left with a purely algebraic problem. The results for this simplified situation say that indeed both types of defects are attractors for the geodesic lines.

Clearly, one has to choose the field configuration in such a way that the geodesics are not turning out of the 2-manifold in question. But this is guaranteed automatically in the case of an SO(3) symmetric gauge field, where the 2-manifold is reducible to a 2-plane containing the SO(3) symmetry axis.

III. SO(3) Symmetric Configurations

Surely, it will be advisable for the discussion of the geodesic problem to restrict oneself to some prototype of gauge field which, on the one hand, is simple enough to be treated exactly and, on the other hand, is able to exhibit the various types of defects. Therefore we shall concentrate our interest exclusively upon SO(3) symmetric field configurations, which essentially makes the problem two-dimensional. In this case one can exploit the properties of complex mappings in order to manage the difficulties with the defect points. Further, the emergence of topological charges may be easily visualized by means of the defects of the two-dimensional characteristic network.

In the following, we shall briefly collect some results of the previous papers and adapt them to the

SO(3) symmetric case. By the way, this procedure is intended to make the present considerations self-contained as far as possible. However, for the basic notions the reader is refered to the preceding papers [1–3].

III.1. Yang-Mills Equations

From the mathematical point of view, the Yang-Mills equations

$$D^{\mu} F_{i\mu\nu} = 0 \tag{III.1}$$

select a special subset of all the possible trivializable field configurations, which we henceforth shall call the *solutions*. In the following we present a geometric approach to the SO(3) symmetric solutions from a general viewpoint.

The starting point for our geometric approach is the condition of generally covariant constancy for the extrinsic curvature fields **B**, i.e.

$$\mathscr{D}_{\mu} B_{i\nu} \equiv D_{\mu} B_{i\nu} - \Gamma^{\lambda}{}_{\nu\mu} B_{i\lambda} = 0 . \tag{III.2}$$

Here Γ may be considered as the standard connection defining the corresponding Riemann-Cartan structure, which may be associated to any trivializable gauge field. For our subsequent discussion of the SO(3) symmetric solutions it is more convenient to introduce two new objects, $\bar{\bar{\Gamma}}$ and **M**, in place of the standard connection Γ, such that the central equation (III.2) reads [1]

$$D_{\mu} B_{i\nu} = \bar{\bar{\Gamma}}^{\lambda}{}_{\nu\mu} B_{i\lambda} + \bar{v}_i M_{\nu\mu} . \tag{III.3}$$

Here, $\bar{\bar{\Gamma}}$ is the conformally flat connection defined through

$$\begin{aligned} \bar{\bar{\Gamma}}^{\lambda}{}_{\nu\mu} &= g^{\lambda}{}_{\nu} q_{\mu} + g^{\lambda}{}_{\mu} q_{\nu} - g_{\nu\mu} q^{\lambda}, \quad \text{(a)} \\ q_{\mu} &= \chi^{-1} \partial_{\mu} \chi . \quad \text{(b)} \end{aligned} \tag{III.4}$$

Further, we have used the generating section $\bar{v}$ in equation (III.3), which lives in the reduced tangent bundle $\bar{\tau}_4$ and is normalized to unity ($\bar{v}^i \bar{v}_i \equiv -1$).

Clearly, in the SO(3) symmetric case we will identify $\bar{v}$ with the normalized position vector $\left(\bar{v}^i \equiv \bar{x}^i = \dfrac{x^i}{r}\right)$ such that the unit normal $\hat{\mathbf{n}}$ of the representative distribution $\bar{\Delta}$ may be decomposed with respect to the "time" unit vector $\hat{t}$ and the "space" unit vector $\hat{\mathbf{r}} = \{0, \bar{x}\}$ as follows:

$$\hat{n}^{\mu} = \hat{t}^{\mu} \cos \varkappa + \hat{r}^{\mu} \sin \varkappa . \tag{III.5}$$

The angular variable $\varkappa$, emerging here, completely characterizes the trivializable field configuration and hence determines both objects $\bar{\bar{\Gamma}}$ and **M**: The conformal scale factor χ (III.4 b) is given by

$$\chi = \frac{c}{r} \sin \varkappa \tag{III.6}$$

and, further, if the tensor **M** of equation (III.3) is decomposed as

$$M_{\mu\nu} = h \varphi^2 g_{\mu\nu} + M_{tt} \hat{t}_{\mu} \hat{t}_{\nu} + M_{tr} (\hat{t}_{\mu} \hat{r}_{\nu} + \hat{t}_{\nu} \hat{r}_{\mu}) + M_{rr} \hat{r}_{\mu} \hat{r}_{\nu} , \tag{III.7}$$

then its components are expressed in terms of $\varkappa$ as follows:

$$\begin{aligned} h &= \cot \varkappa \quad \left(\dot{h} \equiv \frac{\partial h}{\partial t},\ h' \equiv \frac{\partial h}{\partial r}\right), \quad \text{(a)} \\ \varphi^2 &= \frac{1 + h^2 - r^2 (\dot{h}^2 + h'^2)}{r^2 (1 + h^2)^2}, \quad \text{(b)} \\ (1 + h^2) M_{tt} &= \frac{1}{r^2} \frac{\partial}{\partial r} (r h) - \ddot{h}, \quad \text{(c)} \\ (1 + h^2) M_{rt} &= -\frac{1}{r} \frac{\partial}{\partial r} (r \dot{h}), \quad \text{(d)} \\ (1 + h^2) M_{rr} &= -\frac{\partial}{\partial r} \frac{1}{r} \frac{\partial}{\partial r} (r h). \quad \text{(e)} \end{aligned} \tag{III.8}$$

It readily will become clear that the objects $\bar{\bar{\Gamma}}$ and **M** contain all the geometric information inherent in any SO(3) symmetric field configuration. For instance, it is instructive to demonstrate how the Yang-Mills equations (III.1) may be extracted exclusively from the tensor **M**. To this end, remember first that the latter equations may be rewritten for trivializable solutions in the following form [3]:

$$D^{\mu} F_{i\mu\nu} = -F_{i\lambda\sigma} T^{\lambda\sigma}{}_{\nu} = 0 . \tag{III.9}$$

The **T** object emerging here is related to the essential part γ

$$\gamma^{\lambda}{}_{\mu\nu} = \hat{P}^{\lambda}{}_{\sigma} \Gamma^{\sigma}{}_{\mu\nu} \tag{III.10}$$

of the standard connection Γ (cf. (III.2)) through

$$T^{\lambda}{}_{\mu\nu} = \gamma^{\lambda}{}_{\mu\nu} - \hat{P}_{\mu\nu} \gamma^{\lambda\sigma}{}_{\sigma} , \tag{III.11}$$

where $\hat{\mathbf{P}}$ is the (Euclidean) projector orthogonal to $\hat{\mathbf{p}}$. Therefore it is evident that the field equations (III.9) may be recast into some condition upon **M** if we succeed to express γ in terms of **M**.

On behalf of the action of $\hat{\mathbf{P}}$ upon the **B** fields

$$B_{i\lambda} \hat{P}^{\lambda}{}_{\nu} = B_{i\nu} , \tag{III.12}$$

(III.2) may be resolved for the essential part, which yields

$$\gamma^{\lambda}{}_{\mu\nu} = c^2(\mathscr{B}^{-1})^{\lambda\sigma} B^{i}{}_{\sigma}(D_{\nu} B_{i\mu}) . \tag{III.13}$$

The inverse of the fibre metric $\mathscr{B}$ is denoted here by $\mathscr{B}^{-1}$, i.e.

$$(\mathscr{B}^{-1})^{\mu}{}_{\nu}\, \mathscr{B}^{\nu}{}_{\lambda} = \hat{P}^{\mu}{}_{\lambda} . \tag{III.14}$$

Some simple considerations show that the extrinsic curvature **B** for an arbitrary SO(3) symmetric field configuration is given by

$$B_{i\mu} = \bar{v}_i\, b_{\mu} + \frac{\varkappa}{c} \tilde{P}_{i\mu} . \tag{III.15}$$

Here **b** is the gradient (II.18 b) of the angular function $\varkappa$, and $\tilde{\mathbf{P}}$ is the projector onto that 2-dimensional subdistribution $\tilde{\mathbf{\Delta}}$ of the characteristic distribution $\hat{\mathbf{\Delta}}$, which is specified by its (unit)normal $\hat{\mathbf{b}} \in \hat{\mathbf{\Delta}}$.

After these preparations, the essential part γ (III.13) can now be expressed in terms of the tensor **M** as follows:

$$\gamma^{\lambda}{}_{\mu\nu} = \hat{P}^{\lambda}{}_{\sigma}\, \bar{\bar{\Gamma}}^{\sigma}{}_{\mu\nu} - \frac{\hat{b}^{\lambda}}{b} M_{\mu\nu} . \tag{III.16}$$

Further, the tensor **T** (III.11) may now be expressed in terms of **M** via (III.16), where the result suggests the splitting of **T** into two parts, namely

$$T^{\lambda}{}_{\mu\nu} = {}^{(1)}T^{\lambda}{}_{\mu\nu} + {}^{(2)}T^{\lambda}{}_{\mu\nu} . \tag{III.17}$$

This splitting is chosen in such a way that the first contribution ${}^{(1)}\mathbf{T}$ automatically obeys the Yang-Mills equation (III.9)

$${}^{(1)}T^{\lambda}{}_{\mu\nu} = S^{\lambda}{}_{\mu\nu} + S^{\lambda}{}_{\mu}\, \hat{p}_{\nu} + S^{\lambda}{}_{\nu}\, \hat{p}_{\mu} + S^{\lambda} \hat{p}_{\mu}\, \hat{p}_{\nu} , \tag{III.18}$$

whereas the second part ${}^{(2)}\mathbf{T}$ will in general invalidate the field equations

$${}^{(2)}T^{\lambda}{}_{\mu\nu} = -\frac{\hat{b}^{\lambda}}{b} \{\tilde{M}_{\mu\nu} - M^{\sigma}{}_{\sigma} \tilde{P}_{\mu\nu}\} , \tag{III.19}$$

$$(\tilde{M}_{\mu\nu} := \tilde{P}^{\varrho}{}_{\mu} M_{\varrho\sigma} \tilde{P}^{\sigma}{}_{\nu}) .$$

Later on we will see the geometric meaning of the totally symmetric objects **S** occurring in the first part ${}^{(1)}\mathbf{T}$ (III.18).

Now let us return to the original problem concerning the Yang-Mills equations (III.9). Whereas the first part ${}^{(1)}\mathbf{T}$, (III.18), automatically guarantees the validity of these field equations, we must require that the second part ${}^{(2)}\mathbf{T}$, (III.19), vanishes. This yields

$$\tilde{M}_{\mu\nu} = M^{\sigma}{}_{\sigma} \tilde{P}_{\mu\nu} . \tag{III.20}$$

From (III.7) and (III.8) one gets

$$(1+h^2)\left(\ddot{h} + h'' + \frac{h}{r^2}\right) = 3h(\dot{h}^2 + h'^2) . \tag{III.21}$$

This is the Yang-Mills equation for SO(3) symmetric gauge fields of the trivializable type. Though its derivation from the original version (III.1) might appear somewhat lengthy through the introduction of additional geometric objects, we will now need just these objects for the investigation of the geometric properties of the corresponding field configurations.

III.2. Circular Networks

The whole set of trivializable gauge fields may be divided into various classes, where all the field configurations belonging to the same class are sharing the same characteristic surfaces ("characteristic classes"). An important example for such a characteristic class of gauge fields is constituted by the spheroidal configurations, the characteristic surfaces of which are 3-spheres. In the case of SO(3) symmetric configurations, the centers of the 3-spheres must be contained in the SO(3) symmetry axis.

But even within this spheroidal class there exist further subclasses, which may be defined through the shape of the corresponding characteristic lines. The special subclass, in which we are interested for the study of the geodesic problem, is fixed by the requirement that its characteristic lines be circles. Thus, the special subclass mentioned above is represented by two orthogonal systems of circles in the (r, t)-plane ($\bar{E}_2$, say). The motivation for considering such a highly regular network consists in the expectation that the geodesic problem might be solvable exactly in this case.

The starting point for the analysis of the characteristic network is the constancy of the characteristic vector $\hat{\boldsymbol{p}}$ with respect to the standard connection $\mathbf{\Gamma}$:

$$\nabla_{\nu} \hat{p}^{\lambda} \equiv \partial_{\nu} \hat{p}^{\lambda} + \Gamma^{\lambda}{}_{\mu\nu}\, \hat{p}^{\mu} = 0 . \tag{III.22}$$

If, in place of $\mathbf{\Gamma}$, the tensor **T**, (III.11), is used in this relation, the decomposition of the first part ${}^{(1)}\mathbf{T}$, (III.18), yields

$$\partial_{\nu} \hat{p}^{\lambda} = S^{\lambda}{}_{\nu} + S^{\lambda} \hat{p}_{\nu} . \tag{III.23}$$

Evidently, the second rank tensor $S^{\lambda}{}_{\nu}$ describes the geometric shape of the characteristic surfaces, whereas the torsion vector S^{λ} determines their arrangement relative to each other. Applying this to the spheroidal

configurations mentioned above, we obviously find that $S^{\lambda}{}_{\nu}$, which can be expressed explicitly as

$$S_{\lambda\nu} = -\hat{P}_{\lambda\nu}(\hat{p}^{\sigma} q_{\sigma}) - \hat{b}_{\lambda}\,\hat{b}_{\nu}\,\frac{1}{b}\,(\hat{p}^{\varrho} M_{\varrho\sigma}\,\hat{b}^{\sigma})\,, \quad \text{(III.24)}$$

must be proportional to the characteristic projector $\hat{\mathbf{P}}$, which yields the condition

$$\dot{h}\,h'\left(\ddot{h} - h'' - \frac{2}{r}\,h'\right) = (\dot{h}^2 - h'^2)\,\frac{1}{r}\,\frac{\partial}{\partial r}\,(r\,\dot{h})\,. \quad \text{(III.25)}$$

Of course it is very hard to solve this equation directly, when looking for the general spheroidal configurations. However, we shall obtain a special solution below by considering the problem from a different approach.

However, the sphere condition (III.25) is of some help when one analyzes the asymptotic behaviour in the vicinity of a topological point defect. For such a point defect on the symmetry axis ($r=0$) at $t=t_1$ one expects the function $h(t, r)$ to be of the following asymptotic shape:

$$h|_{r\to 0} \;\to\; \frac{H(t)}{r}\,. \quad \text{(III.26)}$$

But now the sphere condition (III.25) demands

$$\ddot{H}|_{t\to t_1} \to 0\,. \quad \text{(III.27)}$$

Moreover, the radius $\varrho_{(3)}$ of the characteristic surface is deduced quite generally from (III.24) as [11]

$$\varrho_{(3)}^{-1} = \frac{\dot{h}}{r\sqrt{\dot{h}^2 + h'^2}}\,. \quad \text{(III.28)}$$

Thus, the asymptotic expansion (III.27) correctly yields the radius of the characteristic surfaces as

$$\varrho_{(3)} = \sqrt{r^2 + (t-t_1)^2}\,, \quad \text{(III.29)}$$

which says that the characteristic spheres indeed collapse onto the topological point defect at $t=t_1$. Simultaneously, it becomes evident from this argumentation that the point defect carries a non-vanishing topological charge. Generalizing this result, one concludes that the topological defects of an arbitrary field configuration with the asymptotic behaviour (III.26) will be determined by the zeros (t_n) of the *defect function* $H(t)$. Furthermore, if the field configuration is required to satisfy the Yang-Mills equations (III.21), we must additionally have $\dot{H}(t_1)^2 = 1$ in (III.27) (single meron solution). More generally, the defect function H will satisfy

$$H(t_n) = 0\,, \quad \dot{H}^2(t_n) = 1\,. \quad \text{(III.30)}$$

Here the relative signs of $\dot{H}(t_n)$ just agrees with the corresponding signs of the topological charges located at the zeros t_n. This is the *local* version of the *global* sphere condition (III.25). The conditions (III.26), (III.30) may now be looked at as the criterium for the presence of meron-like point defects in the general field configuration $h(t, r)$.

Similarly, for the curvature radius $\varrho_{(1)}$ of the characteristic lines one finds

$$\frac{1}{\varrho_{(1)}} = \frac{(\dot{h}^2 h'' + h'^2 \ddot{h}) - 2\,\dot{h}\,h'\,\dot{h}'}{(\dot{h}^2 + h'^2)^{\frac{3}{2}}}\,. \quad \text{(III.31)}$$

Therefore, if it is true that the characteristic lines ($h=\text{const}$) be circles, the right-hand side of (III.31) must exclusively be representable by the function $h(t, r)$ itself.

We are going to give now a simple realization of all the geometric effects discussed so far.

IV. Generalized Dimeron Configurations

Now we want to construct a concrete SO(3)-symmetric configuration in order to demonstrate the essential peculiarities of the geodesic motion in a trivializable gauge field. Some aspects of the geodesic problem in the very special case of the exact dimeron solution have already been discussed in a preceding paper [3]; but that situation was surely too restricted because it included only the topological type of defect.

For this reason, we shall slightly generalize the previous dimeron configuration such that we have now three parameters at hand, (r_S, t_S, h_S), the variation of which allows us to switch on and off both types of defects.

By its very definition, a circular network exclusively consists of circles and therefore surely represents a highly regular structure. Surely, such a regular feature will show up in all the geometric objects; i.e. we try for the tensor $\mathbf{M}$, cf. (III.7),

$$M_{\mu\nu} = h\,\varphi^2\,g_{\mu\nu}\,. \quad \text{(IV.1)}$$

Using here the decomposition (III.7) and (III.8), one is lead to a system of linear differential equations for h, the general solution of which can easily be found to be

$$h(t, r) = \frac{H(t)}{r} + \frac{h_S}{2\,r_S}\,r \quad \text{(IV.2)}$$

with the time-dependent defect function

$$H(t) = \frac{h_S}{2r_S}((t-t_S)^2 \mp r_S^2)\,. \tag{IV.3}$$

This solution depends on three geometric parameters (r_S, t_S, h_S), and there are either two charged point defects or none in agreement with the number of real zeros of the defect function $H(t)$ depending on the choice of sign in (IV.3). Accordingly, the upper (lower) sign will refer henceforth to the charged (uncharged) configuration. If existing, the two topological defects are then situated at

$$t_{1/2} = t_S \pm r_S\,. \tag{IV.4}$$

It is instructive to see how the well-known dimeron solution is contained in the larger set of configurations (IV.2), (IV.3). If the general function $h(t, r)$ is required to satisfy the Yang-Mills equations (III.21), then it follows from a combination of (III.20) and (IV.1) that the function φ (III.8 b) must vanish. Consequently, the Yang-Mills equations select those charged configurations from the larger set which have $h_S = 1$. The characteristic network of the charged configurations is fixed exclusively by the positions $t_{1/2}$ (IV.4) of the topological defects, i.e. by the two parameters (r_S, t_S). Therefore the third parameter (h_S) describes a subclass of gauge fields which belong to the same characteristic network. The Yang-Mills equations then select a special configuration of this subclass by fixing the remaining free parameter $(h_S = 1)$. Clearly, these are the well-known dimeron solutions, where the topological defects at $t_{1/2}$ (IV.4) then agree with the meron centers. The sign of $\dot{H}$ is opposite at the two defects, such that the present solution describes a meron/antimeron system.

It is also obvious from the present arguments that one cannot find a solution among the uncharged configurations. Although the latter ones do not contain topological defects and therefore appear to be more regular than the charged configurations, they nevertheless are not completely free of defects at all. Rather, a change of the parameters (r_S, t_S, h_S) which converts the charged configuration into the uncharged one, simultaneously transforms the topological defects into those of the geometric type. This becomes more evident when looking at the *characteristic networks* of both configurations which provide us with a simple possibility to recognize the type of the defects present in a given configuration: Since the characteristic lines are identical to the fluxlines of the Gauß current **j**, which measures the topological charge Q of any defect, a non-vanishing Q must show up as a sink or source of the Gauß flux. On the other hand, a defect of the geometric type is expected to appear as a vortex-like structure.

For instance, the generalized dimeron configuration (IV.2) with the defect function (IV.3) indeed exhibits a characteristic network of the circular type whose Gauß flux lines turn out as

$$(t-t_S)^2 + \left(r - r_S\frac{h}{h_S}\right)^2 = r_S^2\left(\left(\frac{h}{h_S}\right)^2 \pm 1\right). \tag{IV.5}$$

Here, h is to be considered as a constant which parametrizes the system of circles (h=const). For the charged configurations (see upper sign in (IV.5)), their radius can never be zero, which immediately excludes the emergence of a vortex. All the circles are running through the two topological defects (Figure 1 a). Therefore the latter ones appear as sources/sinks for the Gauß flux, which implies the presence of non-vanishing topological charges.

On the other hand, the radius shrinks to zero for $h \to h_S$ in the case of the uncharged configurations (lower sign in (IV.5)). This implies the emergence of a vortex structure around that submanifold $S \subset E_4$, where the function h takes its extremal value (h_S). Obviously, the defect manifold S is a 2-sphere of radius r_S which is centered at t_S on the symmetry axis (Figure 1 b).

Once the flux lines are known, the characteristic surfaces may be deduced from them by some simple geometric considerations. For the present spheroidal case, they clearly must be 3-spheres

$$(t-(t_S-\delta))^2 + r^2 = \delta^2 \mp r_S^2 \tag{IV.6}$$

being parametrized here by δ.

On the other hand, the *representative surfaces* are determined as solutions of the differential equation (cf. (III.8 a))

$$\frac{\mathrm{d}t}{\mathrm{d}r} = -\frac{1}{h}\,. \tag{IV.7}$$

The special shape (IV.2) for the function h immediately yields the solution

$$2\int_{-\infty}^{t} H(t')\exp\left(\frac{h_S t'}{r_S}\right)\mathrm{d}t' + r^2\exp\left(\frac{h_S t}{r_S}\right) = \Delta^2, \tag{IV.8}$$

where the constant Δ again parametrizes the system of surfaces. Substituting here for H the generalized

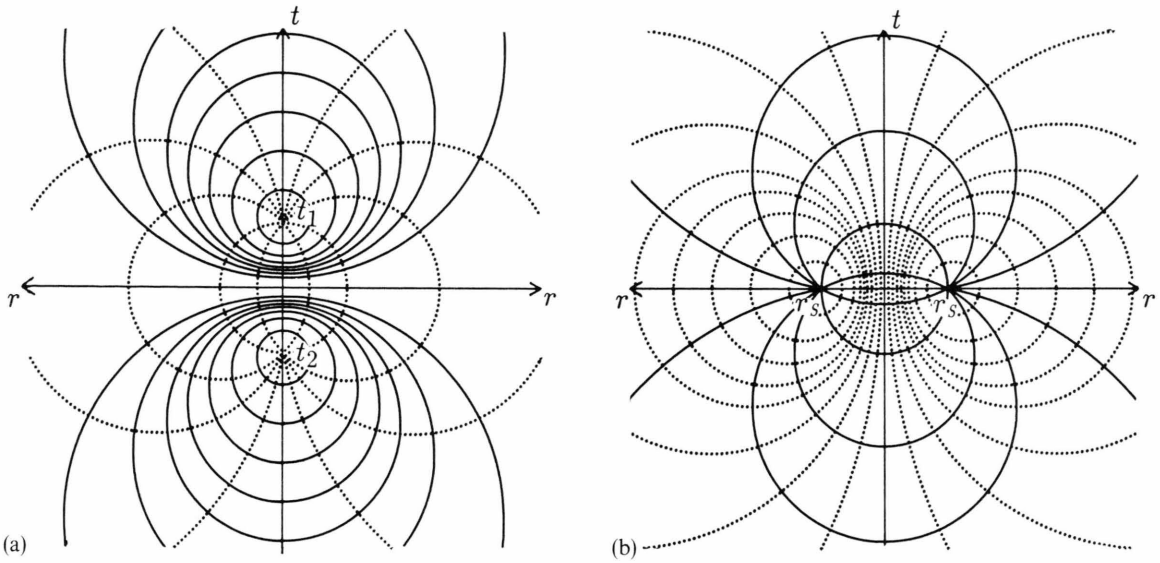

Fig. 1. Characteristic network. For the charged configurations (Fig. 1 a), all characteristic lines (dotted) intersect in the two point defects at $t_{1/2}$, which therefore appear as sources/sinks for the Gauß flux. Correspondingly, the characteristic surfaces (solid) asymptotically collapse onto these defect points. For the uncharged configurations (Fig. 1 b) all the characteristic surfaces (solid) contain the defect manifold S which is a 2-sphere S^2 of radius r_S. This fact prevents the characteristic 3-spheres from collapsing onto a single point, thus excluding the existence of topological defects. However the characteristic lines (dotted) collapse onto a point of the defect manifold S, which signals a vortex structure being typical for the geometric defect.

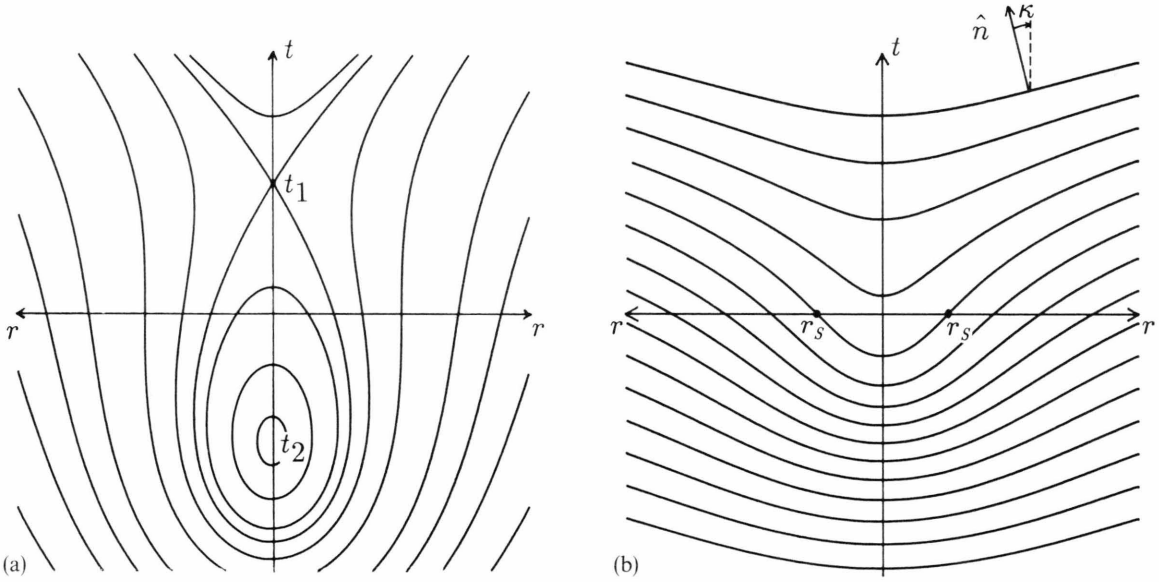

Fig. 2. Representative surfaces. For the charged configuration they are approximated by 3-ellipsoids in the limit $t \to t_2$ (Fig. 2 a, corresponding to Fig. 1 a, $h_S = 0.4$) which become 3-spheres in case of the exact dimeron solution (i.e. $h_S = 1$). In contrast to the topological defects the geometric defects of the uncharged configuration occur in an evidently smooth arrangement of the representative surfaces (Fig. 2 b, corresponding to Fig. 1 b)! The defect manifold S (with radius r_S) consists of those points which carry an extremal value ($\varkappa_S$) of the angular variable $\varkappa$ (III.5). Since the vector $\boldsymbol{b}$ (II.18 b) vanishes on S the fibre metric $\mathscr{B}$ unavoidably becomes degenerate there.

dimeron configuration (IV.3) yields the equation

$$\left(t-\left(t_S+\frac{r_S}{h_S}\right)\right)^2+r^2 = \Delta^2\exp\left(-\frac{h_S t}{r_S}\right)-\left(\frac{r_S}{h_S}\right)^2[1\mp h_S^2], \qquad \text{(IV.9)}$$

which obviously is a generalization of the dimeron surface (upper sign, $h_S=1$) previously studied [1]. A simple consideration of the asymptotic behaviour of the representative surface around the defects gives an interpretation to the parameters h_S: it measures the deviation of the representative surfaces from the asymptotic spherical (hyperboloid) shape ($h_S=1$), which in this way is singled out by the Yang-Mills equations. Observe here that the *characteristic surfaces* are 3-spheres in any case!

Next, consider the uncharged configurations (Figure 2b). The corresponding 3-surfaces being completely regular, one would not have supposed that there is a defect in this structure. The defect manifold S is defined through the extremal value $\varkappa_S$ of the angle of the normal $\hat{\mathbf{n}}$ of $\bar{\Delta}$ with respect to the SO(3) symmetry axis, i.e.

$$\dot{h}(r_S, t_S) = h'(r_S, t_S) = 0\,. \qquad \text{(IV.10)}$$

If one insists on the boundary condition of asymptotically flat 3-sheets far away, such a defect of the geometric type can obviously be avoided only by admitting topological defects. This however means that we cannot have configurations which are completely free of both types of defects and simultaneously obey the asymptotic flatness condition! Quite on the contrary, the general configuration will exhibit even both types of defects.

In a general mixed configuration the situation becomes even more complicated because the geometric type of defects can split into further subclasses. Since the linear term of a Taylor expansion of h around a geometric defect point vanishes, the shape of the characteristic lines $h=\text{const}$ then is determined by the quadratic term. The adequate mathematical apparatus for a more rigorous treatment of this sort of problems is the *Morse theory* [12]. In terms of this theory, a geometric defect point in the (r, t)-plane is a *critical point* of the angular function $\varkappa(t, r)$. Restricting ourselves to non-degenerate critical points, the *elliptic* and *hyperbolic* defects differ with respect to their *Morse index* (0 or 1). Unfortunatelly the well-known Morse inequalities are not applicable here in order to estimate the number of elliptic and hyperbolic defects for a given set of topological charges. The reason is that the Morse inequalities are valid only for compact manifolds, whereas the excision of the topological defect points from the (r, t)-plane leaves a non-compact space.

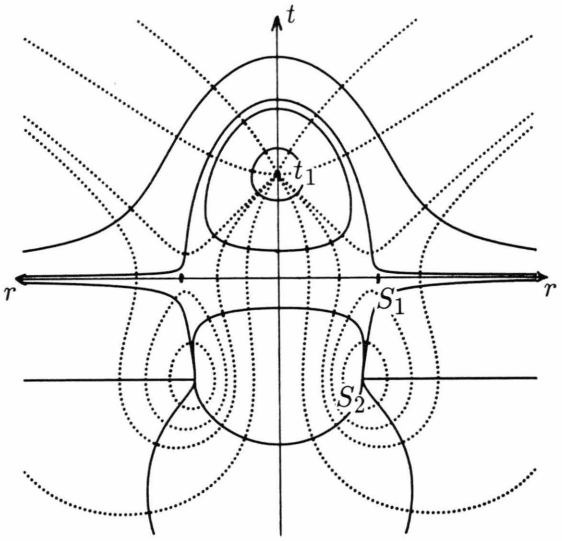

Fig. 3. Characteristic network of mixed defects. The presence of a single topological defect (at t_1) causes the simultaneous occurrence of both types of geometric defects (S_1 and S_2). The reason is that any flux line (dotted) emanating from the point charge ultimately must extend to infinity in order to produce the correct value of the topological charge integral Q (II.13).

As a simple demonstration of a mixed configuration consider the defect function (Fig. 3)

$$H(t) \to {}^{(1)}H(t)\,{}^{(2)}H(t)\,, \qquad \text{(IV.11)}$$

where ${}^{(1)}H(t)$ is a first-degree polynomial and ${}^{(2)}H(t)$ is of the dimeron form (IV.3). Here the geometric defect manifolds are again 2-spheres surrounding the symmetry axis but, in contrast to the uncharged generalization of the dimeron configuration, the characteristic lines around one of them (S_1) are hyperbolas rather than circles. Physically speaking, such a defect acts repulsively rather than attractively upon the characteristic geodesics.

V. Geodesics

A complete solution of the global geodesic problem for the preceding field configuration is obtainable if one restricts the motion of the test particles to a 2-plane

containing the SO(3) symmetry axis ((r, t)-plane). The reason is that the restriction of the Riemannian curvature 2-form onto this plane vanishes such that the Riemannian problem may reduced to its Euclidean analogue. Consequently, one merely has to pull back the Euclidean geodesics to the (r, t)-plane. Thus, one is not forced to really integrate the geodesic equation (II.16) but rather one is left with a simple algebraic problem. Moreover, the pull back method gives a mathematical explanation why the topological and elliptical defect points are always attractive, independent of the choice of the integrating factor.

V.1. Plane Geodesics

Consider the restriction of the general Riemannian line element (ds) onto the (r, t)-plane $\bar{E}_2$, which may be thought to be spanned by $\hat{\boldsymbol{p}}$ and $\hat{\boldsymbol{b}}$:

$$ds^2 = -G_{\mu\nu}\, dx^\mu\, dx^\nu|_{\bar{E}_2} = c^2(b_\mu\, dx^\mu)^2 + (p_\mu\, dx^\mu)^2 . \quad \text{(V.1)}$$

Here, the fact may be used that both vectors $\boldsymbol{b}$ and $\boldsymbol{p}$ are gradient fields. Therefore the Riemannian line element (V.1) formally assumes the Euclidean shape when written in terms of the scalares $\varkappa$ and ξ,

$$ds^2 = c^2[(d\varkappa)^2 + (d\xi)^2] . \quad \text{(V.2)}$$

Clearly, such a pleasant result extremely facilitates the geodesic problem because in the $\{\varkappa, \xi\}$-space ($\tilde{E}_2$, say) the geodesics are straight lines which can be parametrized (at least piecewise) by their arc length s:

$$\begin{aligned} \varkappa(s) &= \varkappa(0) + \frac{\sin\alpha}{c}\, s , \quad \text{(a)} \\ \xi(s) &= \xi(0) + \frac{\cos\alpha}{c}\, s . \quad \text{(b)} \end{aligned} \quad \text{(V.3)}$$

Here, the *characteristic angle* α defines the orientation of the geodesic line relative to the characteristic network. Remember that the latter one is built by the characteristic lines ($\varkappa = \text{const}$) and the characteristic surfaces ($\xi = \text{const}$). Both types of curves are mutually orthogonal as well in $\tilde{E}_2$ as in the real (r, t)-plane $\bar{E}_2$. The geodesic problem is solved principally by inverting the map $f_r: \bar{E}_2 \to \tilde{E}_2$, defined through the functions $\varkappa(t, r)$ and $\xi(t, r)$, which then yields $r = r(\varkappa, \xi)$ and $t = t(\varkappa, \xi)$ with $\varkappa$ and ξ given by the geodesic solution (V.3).

Concerning the potential $\xi(x)$, there are two points which deserve some attention.

(i) As the discussion of the generalized dimeron configuration shows, the characteristic vector field $\boldsymbol{p}$ is ill-defined at the defect points of both types due to their very definition. Therefore the parametrization of the 2-plane $\bar{E}_2$ by means of the new coordinates $\{\xi, \varkappa\}$ will become singular at those defect points S. But the exclusion of these singular points from the $\{\xi, \varkappa\}$-coordinatization leaves a truncated 2-plane $\mathring{E}_2 := \bar{E}_2 \setminus S$, which is no longer simply connected. As a consequence, one has to work with some covering $\mathscr{E} = \{\mathscr{E}(a)\}$ of $\mathring{E}_2$,

$$\mathring{E}_2 = \bigcup_a \mathscr{E}(a) , \quad \text{(V.4)}$$

such that anyone of the 2-patches $\mathscr{E}(a)$ is simply connected and hence admits the construction of a (local) potential ${}^{(a)}\xi(x)$ by means of

$${}^{(a)}\xi(x) = \int_{x(a)}^{x} p_\mu\, dx^\mu \quad (x(a),\ x \in \mathscr{E}(a),\ x(a) \text{ fixed}) . \quad \text{(V.5)}$$

In the intersections $\mathscr{E}_{ab} = \mathscr{E}(a) \cap \mathscr{E}(b)$ the corresponding potentials are the differing by a constant $\mathscr{C}_{ba}$

$${}^{(b)}\xi(x) = {}^{(a)}\xi(x) + \mathscr{C}_{ba} . \quad \text{(V.6)}$$

Now the geodesic construction (V.3) may be performed separately in anyone of the 2-patches $\mathscr{E}(a)$ by local maps ${}^{(a)}f_r$ which then yield all geodesics running through that patch. A general geodesic, extending over an arbitrary large part of $\mathring{E}_2$, will then be found to be composed by the corresponding local geodesics in a smooth way. However, in special cases it is possible to work with one single function $\xi(x)$ over the whole $\mathring{E}_2$, despite the fact that $\mathring{E}_2$ is multiply connected! This may be feasible if the configuration contains only charged defects where the loop version of the integral (V.5) vanishes whenever the integration path is homotopic to the $\mathring{E}_2$ cut of a characteristic surface (see the example below).

(ii) The second point refers to the non-uniqueness of the integrating factor ψ (II.18a). By assumption, the characteristic unit vector $\hat{\boldsymbol{p}}$ is well-defined off the defect set S, and hence it will produce there a non-degenerate, well-defined metric $\mathbf{G}$ (II.1) provided the integrating factor ψ vanishes nowhere. Clearly, one will take advantage of this arbitrariness of ψ by trying to use only those functions ψ which are non-zero everywhere in order to keep the Riemannian metric $\mathbf{G}$ regular off the defect set S.

Returning to the generalized dimeron configuration, consider for example a potential (ξ_I, say) which is a unique function of the curvature radius $\varrho_{(3)}$

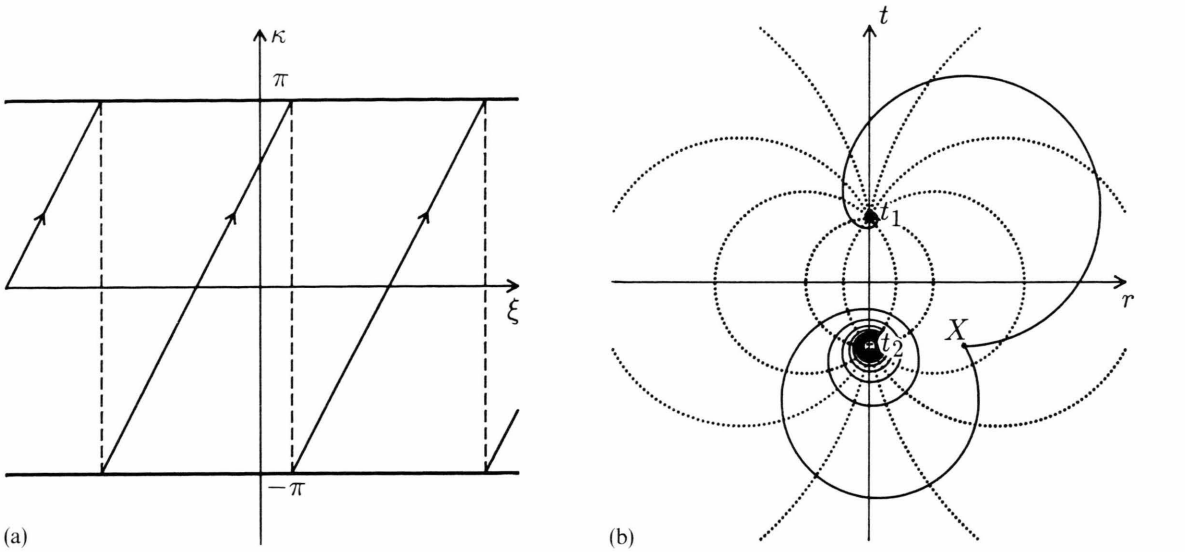

Fig. 4. Geodesics for the charged configuration. The geodesics (Fig. 4b, solid lines; dotted: characteristic lines) due to the potential ξ_I (V.7) are simply the pullback to the (r, t)-plane of the straight lines in the $(\varkappa, \xi)$-plane (Figure 4a). The topological charges are acting as attractors for the geodesic lines independent of the initial conditions (starting point: X).

(III.28). Choosing

$$\xi_I = \frac{c}{\varrho_{(3)}}, \quad c = \text{const} \tag{V.7}$$

one finds

$$\xi_I = \frac{c\dot{h}}{\sqrt{h^2 \pm h_S^2}}, \tag{V.8}$$

and hence the corresponding factor (ψ_I) becomes

$$\psi_I = -c\,\hat{p}^\mu \partial_\mu \xi_I = c^2 \frac{h_S}{r_S} \frac{r\dot{h} \pm r_S h_S}{r_S r^2 (h^2 \pm h_S^2)}. \tag{V.9}$$

However, for the uncharged configuration this factor ψ_I vanishes just at the "minimal" characteristic surface ($\delta = 0$ in (IV.6)) whereas it remains nonzero everywhere in $\mathring{E}_2$ for the charged configuration! Thus, our conclusion is that the potential ξ_I (V.7) generates a regular Riemannian structure over $\mathring{E}_2$ for the charged configuration but not for the uncharged one! We will overcome this lack later by utilizing the non-uniqueness of ξ. At the moment we restrict ourselves to a discussion of the charged case only.

Since the analytic expressions for f_r and f_r^{-1} are somewhat unwieldy, we do not want to reproduce them here. Rather, we prefer to discuss f_r by means of a diagram (Figure 4a). Since the angle $\varkappa$ is bounded, the image of $\bar{E}_2$ in $\tilde{E}_2$ is a strip defined through $\{-\pi \leq \varkappa \leq \pi;\ -\infty < \xi < \infty\}$, where the upper $(\varkappa = +\pi)$ and the lower $(\varkappa = -\pi)$ boundaries have to be identified. This generates the topology of a 2-cylinder, and thus the map f_r acquires a semi-compactifying property. Correspondingly, the circumference in $\bar{E}_2$ of any characteristic surface ($\xi = \text{const}$) has always the same Riemannian length $\overset{*}{L}_{CS} = 2\pi c$.

The geodesics (V.3) are piecewise straight lines in $\tilde{E}_2$, which may be continued forward and backward and then evidently extend to infinity along the non-compactified dimension. However, the infinite points $\xi_I = \pm\infty$ correspond to the meron positions $\{0, t_{1/2}\}$, respectively, in $\bar{E}_2$. Therefore, any plane geodesic starting with an initial angle $\alpha \neq \frac{\pi}{2}$ necessarily terminates at one of the two point defects. Only for $\alpha = \frac{\pi}{2}$ the test particle moves on the circumference of a characteristic 3-sphere ($\xi = \text{const}$) and therefore avoids plunging into a topological defect. Moreover, the infinitely many reflections of the geodesic at the strip boundaries imply that the test particle approaches a topological defect by an infinite number of revolutions along a spiral line (Figure 4b). Consequently, the proper life time of the particle is infinite ($\overset{*}{L}_{GL} = \infty$), where we have freely identified the Riemannian arc length of a geodesic (GL) with the "proper time" of the "test paricle". Obviously, the question of a finite/infinite lifetime is strongly related to the semi-compactifying property of the map f_r!

Summarizing our results, we see that the most striking feature of the topological defect consists in its attractive action upon a test particle moving along a geodesic line.

V.2. The Non-Uniqueness of the Riemannian Connection

For a given trivializable gauge field, the Riemannian connection $\mathbf{\Gamma}$ is not fixed uniquely, whereas its projection γ onto the characteristic distribution can be calculated immediately from (III.13). This ambiguity corresponds to the non-uniqueness of the potential ξ (resp. the integrating factor ψ) which determines the **p**-component of the metric (V.1). Of course we are interested mainly in those features of the Riemannian structure which are invariant with respect to the allowed changes of ξ. Especially we want to investigate the invariants referring to the geodesic motion of a test particle. Here, we shall use the results of the preceding section for the comparison with a different choice (ξ_{II}) for the potential. This comparison then yields a demonstration of the invariants.

The starting point for a discussion of the ambiguity of ψ is the decomposition of its gradient into the torsion vector **S**, cf. (III.23), and the characteristic vector $\hat{\boldsymbol{p}}$ according to

$$\psi^{-1}\hat{\partial}_\mu\psi = S_\mu + \Phi\hat{p}_\mu\,. \tag{V.10}$$

The scalar Φ emerging here enters the theory via the Frobenius integrability theorem [3] and is easily seen to be non-unique. This non-uniqueness is then transferred immediately to the factor ψ, i.e. any given ψ may be equally well replaced by a modified ψ,

$$\psi \to \psi\beta\,, \tag{V.11}$$

where the scalar β is constant on the characteristic surfaces

$$\hat{\partial}_\mu\beta \sim \hat{p}_\mu\,. \tag{V.12}$$

This fact forces us to make a decision about which ψ should be used for the computation of the geodesic trajectory. Moreover, one wants to see the geometric meaning of the indeterminacy of ψ.

For the dimeron solution ($h_S=1$) the tensor **M** (III.7) vanishes identically, which makes it possible to identify the required connection in that special case with the conformally flat connection $\bar{\mathbf{\Gamma}}$ by means of (III.3, III.4). Such a choice $\psi\equiv\chi$ is not possible in general. Rather, one will try the ansatz

$$\psi = \chi\cdot\lambda \tag{V.13}$$

by introducing some correction factor λ. From (V.11) and (V.12) we know that the component of the gradient $\hat{\partial}_\mu\lambda$ along the characteristic vector $\hat{\boldsymbol{p}}$ merely generates a change of ψ according to (V.11).

Therefore, one may try to put this component equal to zero:

$$\hat{p}^\mu\hat{\partial}_\mu\lambda = 0\,. \tag{V.14}$$

This requirement yields the new integrating factor

$$\psi_{II} = \frac{c\,h_S}{r}(h^2 \pm h_S^2)^{-1/2} \tag{V.15}$$

which does not change sign and therefore does not suffer from the lack of its predecessor ψ_I (V.9).

The corresponding potential is obtained by considering equation (II.18 a) as a differential equation for $\xi_{II}(t, r)$. This equation is found to be of the well-known Cauchy-Riemann form

$$\begin{aligned} &\frac{\partial\xi_{II}}{\partial t} = -\frac{\partial\eta}{\partial r}, \quad \text{(a)} \\ &\frac{\partial\xi_{II}}{\partial r} = \frac{\partial\eta}{\partial t}, \quad \text{(b)} \end{aligned} \tag{V.16}$$

where the function η is given by

$$\eta = \left\{\begin{array}{l} \operatorname{arccot}\left(\dfrac{h}{h_S}\right) \\[2ex] \operatorname{ArCoth}\left(\dfrac{h}{h_S}\right) \end{array}\right\} \tag{V.17}$$

for the charged/uncharged configurations, respectively. The Cauchy-Riemann equations (V.16) guarantee the existence of a conformal map $f_c\colon {}^c\bar{E}_2 \to {}^c\tilde{E}_2$ which takes the (complexified) (r, t)-plane ${}^c\bar{E}_2$ into the (ξ, η)-plane ${}^c\tilde{E}_2$ such that

$$\zeta \equiv \xi + i\eta = f_c(z) \in {}^c\tilde{E}_2\,, \quad (z := r + it \in {}^c\bar{E}_2). \tag{V.18}$$

Thus the characteristic lines ($\eta=$const.) and the ${}^c\bar{E}_2$ circumferences ($\xi=$const.) of the characteristic surfaces are mapped *conformally* into the orthogonal network of straight lines parallel to the coordinate axes of ${}^c\tilde{E}_2$. The potential ξ_{II} may easily be found from (V.16) by a simple integration as

$$\xi_{II}(t, r) = \left\{\begin{array}{l} \operatorname{ArTanh}\left(\dfrac{r\dot{h}}{\dfrac{r}{r_S}h + h_S}\right) \\[2ex] \arctan\left(\dfrac{r\dot{h}}{\dfrac{r}{r_S}h - h_S}\right) \end{array}\right\}. \tag{V.19}$$

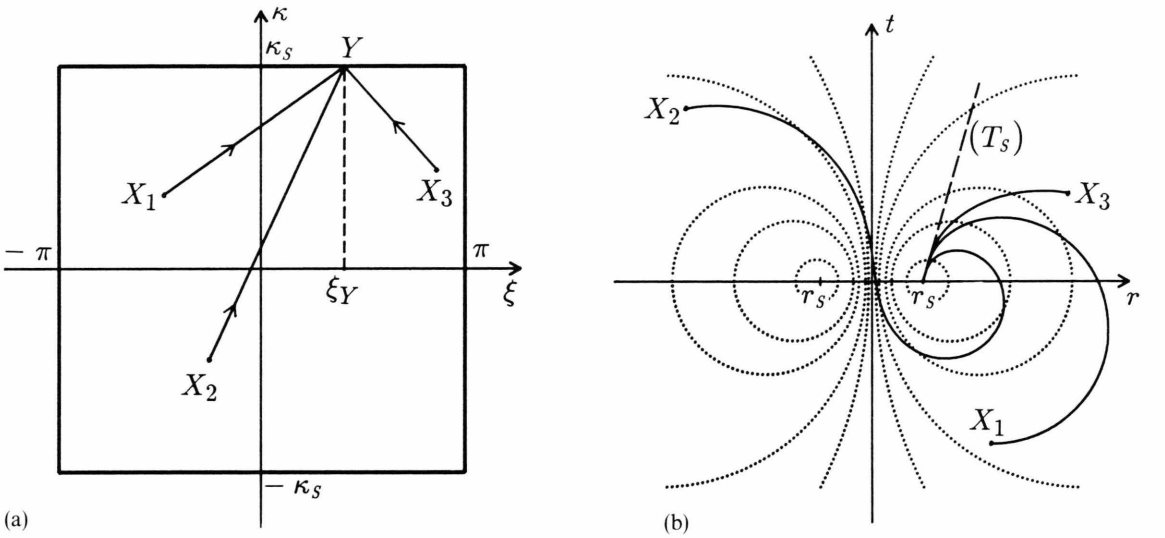

Fig. 5. Geometric defects as attractors. The covering of $\mathring{E}_2$ with the 2-patches, cf. (V.23), generates a discontinuity of the function ξ in the overlap region ($t=t_S$, $r=r_S$) which implies the identification of the points ($\xi=\pm\pi$, $\varkappa$). This gives to the allowed region ($-\varkappa_S<\varkappa<+\varkappa_S$, $-\pi\leq\xi\leq+\pi$) the geometry and topology of a cylinder (Fig. 5a), where the boundaries ($\varkappa=\pm\varkappa_S$) act as attractors for the geodesic lines. The pullback f_r^{-1} to $\mathring{E}_2$ gives the geodesics in real space (Fig. 5b), which then must necessarily terminate at the geometric defects of the elliptic type. A point Y of the horizontal boundary ($\varkappa=\pm\varkappa_S$) fixes the direction (ξ_Y) of the tangent to all geodesics starting from arbitrary points X and terminating at the elliptic defect ($\varkappa=\varkappa_S$) with the same tangent. For a given tangent (T_S) at the defect point, there is a geodesic terminating at the defect point with (T_S) and starting from an arbitrary point X of the (r, t)-plane $\mathring{E}_2$.

Here, it is worth while to spend a moment upon the special situation when the Yang-Mills equations are satisfied ($h_S=1$). In this case, the imaginary part η (V.17) of ζ becomes proportional to the angle $\varkappa$ (III.8a) itself. On the other hand, both ξ and η are always harmonic functions,

$$\ddot{\xi}+\xi''=\ddot{\eta}+\eta''=0\,, \tag{V.20}$$

so that for $h_S=1$ this statement transfers to the angle $\varkappa$,

$$\ddot{\varkappa}+\varkappa''=0\,. \tag{V.21}$$

Of course, this simple result holds only for the dimeron solution and was already observed in a former paper [1], but the present arguments may give a hint that also for the multimeron solution there could exist a function $\eta(\varkappa)$ obeying the 2-dimensional Laplace equation.

V.3. Topological Invariant of the Geodesics

Returning to the general case ($h_S\neq 1$) the geodesic problem for the charged configuration (upper case in (V.19)) is qualitatively quite similar to the previous choice ξ_I (V.8), as illustrated by Fig. 4, and therefore the results need not be presented here in detail. Especially the main result is exactly the same: the topological charges act as attractors for the geodesic lines, which all must ultimately terminate at those topological point defects. This fact is readily established by observing that the new potential ξ_{II} (V.19) is a function of the old one ξ_I (V.7) with the topological defects corresponding to the fix points of the map $\xi_I\to\xi_{II}$:

$$\xi_{II}=\mathrm{ArSinh}\left(\frac{r_S\,\xi_I}{c}\right)\quad\text{(charged configuration)}. \tag{V.22}$$

However the uncharged configuration (lower case in (V.17), (V.19)) presents some features which are worth while to be discussed in some length. First, observe here that one can no longer deal with a single function $\xi(t, r)$ over the whole 2-space $\mathring{E}_2$. Rather one has to resort to a non-trivial covering $\mathscr{E}$ (V.4) of $\mathring{E}_2$ containing at least two patches $\mathscr{E}(a)$ ($a=1, 2$) with a non-trivial value of the constant $\mathscr{C}_{ba}$, cf. (V.6). The patch construction has to be performed in such a way that the domain of ambiguity of the potential ξ_{II} ((V.19), lower case) is entirely contained in it. The domain of ambiguity becomes immediately obvious by introducing the function $h(t, r)$ (IV.3) into (V.19),

which yields

$$\xi_{II}(t, r) = \arctan\left(\frac{2r_S(t-t_S)}{r^2-r_S^2+(t-t_S)^2}\right) \quad \text{(uncharged configuration)}. \tag{V.23}$$

If this function ξ_{II} is required to be continuous across the inner part ($r<r_S$) of the equatorial 3-plane ($t=t_S$) of the minimal characteristic surface, cf. (IV.6), then it develops a discontinuity of amount 2π across the outer part ($r>r_S$):

$$\lim_{(t-t_S)\to\pm 0} \xi_{II} = \pm\pi, \quad r>r_S\,. \tag{V.24}$$

With this arrangement, the geodesics (V.3) in $\tilde{E}_2$ are to be constructed as shown in Fig. 5a, where the geodesics in $\bar{E}_2$ (Fig. 5b) follow again by inversion of the corresponding map f_r. Obviously, the geometric defects of the elliptic class also act as attractors of all geodesic lines. It follows from Fig. 5a that, in contrast to the analogous situation for the topological defects, the "proper time" for arriving at the defect positions is finite here. Figure 5 also shows that any point of the truncated plane $\mathring{E}_2$ can be connected with an elliptic defect point by a geodesic with an arbitrary prescriped tangent at the defect position. In this way the geodesic problem, admitting normally only one single geodesic between two (nearby) points, is spoiled completely. As a result, one does not know which of the infinitely many geodesics, emanating with the same tangent at the defect point, one should choose as the continuation of the given geodesic.

The present results clearly reveal now the topological invariants of the geodesics with respect to some change of the integrating factor ψ, which itself determines the metric properties of the Riemannian structure along the characteristic curves. Any change of the metric $\mathbf{G}$ via ψ may be considered as the transition to a new potential ξ by means of a 1-diffeomorphism, such as for instance given by (V.22). Such a modification of the potential ξ induces a new map f_r of $\mathring{E}_2$ into $\tilde{E}_2$. Since the image regions of $\mathring{E}_2$ in $\tilde{E}_2$ with respect to both maps f_r are diffeomorphic to each other, the geodesics (due to the corresponding metric tensors $\mathbf{G}$) are deformations of each other with the end points (=defects) being fixed.

This is the desired result: *The topological and elliptic defect points of the characteristic network are the attractors of the geodesic curves independently of the choice of the Riemannian structure (via ψ).* Though this result has been derived only for the generalized dimeron configurations, it seems to us that it may hold quite generally. Furthermore it became evident that for any choice of the Riemannian structure the geodesics cannot be continued beyond the defect points without arbitrariness.

[1] R. Brucker and M. Sorg, Z. Naturforsch. **41a,** 571 (1986).
[2] R. Brucker and M. Sorg, Z. Naturforsch. **42a,** 521 (1987).
[3] M. Mattes and M. Sorg, Z. Naturforsch. **44a,** 222 (1989).
[4] A. Held (ed.), General Relativity and Gravitation, Plenum Press, New York 1980, vol. I, p. 23.
[5] M. Mattes and M. Sorg, Il Nuovo Cim. **106B,** 273 (1991).
[6] In the present paper the Riemannian metric is denoted by $\mathbf{G}$, in place of $\overset{*}{\mathbf{G}}$ [3], since there is no need to discern between the Riemann and the Riemann-Cartan cases.
[7] V. De Alfaro, S. Fubini, and G. Furlan, Phys. Lett. **65B,** 163 (1976); ibid. **72 B,** 203 (1977); ibid. **73B,** 463 (1978).
[8] J. Glimm and A. Jaffe, Phys. Lett. **73B,** 167 (1978); Phys. Rev, **D 18,** 463 (1978).
[9] We raise and lower indices with the Euclidean metric and use the signature $g_{\mu\nu}=\mathrm{diag}(-1,-1,-1,-1)$.
[10] A hat on a vector as $\hat{p}$, $\hat{b}$ etc. means Euclidean normalisation i.e. $\hat{p}^\mu\hat{p}_\mu=-1$.
[11] The sign of $\varrho_{(3)}$ gives an orientation to the characteristic surfaces.
[12] C. Nash and S. Sen, Topology and Geometry for Physicists, Academic Press, London 1983.
[13] W. Drechsler, Z. Naturforsch. **46a,** 645 (1991). (Observe the different meaning of some symbols – e.g. $B^i{}_\mu$, $S_{\lambda\mu\nu}$ – in that and our paper.)